From Adiabatic to Dispersive Readout of Quantum Circuits

Sunghun Park,[1] C. Metzger,[2] L. Tosi,[2,3] M. F. Goffman,[2] C. Urbina,[2] H. Pothier,[2] and A. Levy Yeyati[1,4,*]
[1]Departamento de Física Teórica de la Materia Condensada, Condensed Matter Physics Center (IFIMAC), Universidad Autónoma de Madrid, 28049 Madrid, Spain
[2]Quantronics group, Service de Physique de l'État Condensé (CNRS, UMR 3680), IRAMIS, CEA-Saclay, Université Paris-Saclay, 91191 Gif-sur-Yvette, France
[3]Centro Atómico Bariloche and Instituto Balseiro, CNEA, CONICET, 8400 San Carlos de Bariloche, Río Negro, Argentina
[4]Instituto Nicolás Cabrera, Universidad Autónoma de Madrid, 28049 Madrid, Spain

(Received 9 May 2020; accepted 9 July 2020; published 10 August 2020)

Spectral properties of a quantum circuit are efficiently read out by monitoring the resonance frequency shift it induces in a microwave resonator coupled to it. When the two systems are strongly detuned, theory attributes the shift to an effective resonator capacitance or inductance that depends on the quantum circuit state. At small detuning, the shift arises from the exchange of virtual photons, as described by the Jaynes-Cummings model. Here we present a theory bridging these two limits and illustrate, with several examples, its necessity for a general description of quantum circuits readout.

DOI: 10.1103/PhysRevLett.125.077701

Circuit quantum electrodynamics (QED) is at the heart of most advanced superconducting quantum technologies. Different types of superconducting qubits can be strongly coupled to microwave resonators thus achieving regimes and phenomenena which cannot be reached within the realm of quantum optics [1]. More recently, strong coupling between microwave resonators and a variety of other quantum systems not necessarily involving superconductors has been achieved [2], extending further the realm of circuit QED. In all these applications the measurement of the qubit or the hybrid device state is achieved by monitoring the resonator properties. Theoretically, two regimes have been approached using disconnected descriptions [3]: the *dispersive* regime, where the qubit-resonator detuning is larger than the coupling strength yet small enough to allow the exchange of virtual photons, and the *adiabatic* regime, where the detuning is sufficiently large for virtual processes to be strongly suppressed. The dispersive regime, which describes level repulsion between those of the quantum circuit and of the resonator, is typically dealt with using a Jaynes-Cummings Hamiltonian within different levels of approximation [3–10]. In contrast, the adiabatic regime accounts for the renormalization of the resonator capacitance or inductance by the effective capacitance of the circuit, including its "quantum capacitance" [11,12], or its effective inductance [13,14], which modifies the resonator frequency [15,16].

However, there is no actual border between these two regimes which could justify a separate treatment, as illustrated by recent experiments on hybrid circuit QED setups [17] that reveal features of both regimes for the same device. This situation claims for a unified description of quantum circuits readout, going beyond the standard Jaynes-Cummings model, which could be applied to different types of devices over a large range of parameters.

In the present Letter we derive a general expression for the resonator frequency shift when coupled to a generic quantum circuit. This expression naturally interpolates between the adiabatic and the dispersive regimes, thus allowing us to clarify their origin from the same coupling Hamiltonian. In addition, our formalism is not restricted to the usual two-level approximations, and it can describe any multilevel situation on the same footing. We illustrate the importance of the different terms in our expression by analyzing well-known models like a short single channel superconducting weak link hosting Andreev states, the radio frequency SQUID (rf-SQUID) and the Cooper pair box.

Resonator-quantum circuit coupling.—The system we consider comprises a resonant circuit and a quantum circuit coupled through phase or charge fluctuations as depicted in Figs. 1(a) and 2(a) and in the inset of Fig. 3. The resonant circuit is represented as a lumped-element LC resonator with bare resonance frequency $f_r = \omega_r/2\pi$, with $\omega_r = 1/\sqrt{L_r C_r}$. Introducing the photon annihilation (creation) operators a ($a^\dagger$), it can be described by the Hamiltonian $H_r = \hbar\omega_r a^\dagger a$. On the other hand, the quantum circuit Hamiltonian, $\hat{H}_{\rm qc}(x)$, depends on a dimensionless control parameter x, corresponding to an excess charge on a capacitor or a flux through a loop. We denote by $|\Phi_i(x)\rangle$ the eigenstates of the uncoupled quantum circuit, $\hat{H}_{\rm qc}(x)|\Phi_i(x)\rangle = E_i(x)|\Phi_i(x)\rangle$. Flux (charge) fluctuations in the resonator lead to $x \to x_0 + \hat{x}_r$, where $\hat{x}_r = \lambda(sa + s^* a^\dagger)$, with λ a coupling constant depending on the coupling scheme [18], and $s = 1$ $(-i)$. We assume

$\lambda \ll 1$ in accordance with experiments. The resonator-quantum circuit coupling Hamiltonian $\hat{H}_c$ is obtained by expanding $\hat{H}_{\rm qc}(x_0+\hat{x}_r)$ up to second order in $\hat{x}_r$

$$\hat{H}_c(x_0) = \hat{x}_r \hat{H}'_{\rm qc}(x_0) + \frac{\hat{x}_r^2}{2}\hat{H}''_{\rm qc}(x_0), \tag{1}$$

where the prime stands for the derivative with respect to x. The Hamiltonian describing resonator, quantum circuit and their coupling is therefore

$$\hat{H} = \hbar\omega_r a^\dagger a + \hat{H}_{\rm qc}(x_0) + \lambda \hat{H}'_{\rm qc}(x_0)(sa + s^* a^\dagger) + \lambda^2 \hat{H}''_{\rm qc}(x_0)(a^\dagger a + 1/2), \tag{2}$$

where terms $\lambda^2 a^{(\dagger)2}$ leading to corrections of order λ^4 have been neglected. When the quantum circuit is described as a two-level system and the terms involving $H''_{\rm qc}$ in Eq. (2) are neglected, this model corresponds to the well-known Jaynes-Cummings Hamiltonian.

We shall now evaluate, using perturbation theory up to second order in λ, the resonator shift when the quantum circuit is on a given state $|\Phi_i\rangle$. The Hellmann-Feynman theorem establishes that $E'_i = \langle\Phi_i|\hat{H}'_{\rm qc}|\Phi_i\rangle$. Taking the derivative on both sides gives

$$E''_i = \langle\Phi'_i|\hat{H}'_{\rm qc}|\Phi_i\rangle + \langle\Phi_i|\hat{H}''_{\rm qc}|\Phi_i\rangle + \langle\Phi_i|\hat{H}'_{\rm qc}|\Phi'_i\rangle. \tag{3}$$

Here, $|\Phi'_i\rangle = \partial|\Phi_i\rangle/\partial x$ can be expressed as $|\Phi'_i\rangle = -G_i(G_i^{-1})'|\Phi_i\rangle$ where $G_i = (E_i - \hat{H}_{\rm qc})^{-1}$. Substituting this into Eq. (3) and using identity $\sum_i |\Phi_i\rangle\langle\Phi_i| = 1$, we obtain the relation between the diagonal matrix element of $\hat{H}''_{\rm qc}$ and the curvature E''_i of the energy level i,

$$\langle\Phi_i|\hat{H}''_{\rm qc}|\Phi_i\rangle = E''_i + 2\sum_{j\neq i}\frac{|\langle\Phi_i|\hat{H}'_{\rm qc}|\Phi_j\rangle|^2}{E_j - E_i}. \tag{4}$$

Combining this result with the second order correction of the system energy levels arising from the $\hat{H}'_{\rm qc}$ term in Eq. (2) [18], we obtain the shift of the energy of the coupled system when the circuit is in state $|\Phi_i\rangle$ and the resonator contains n photons

$$\delta\omega_{i,n} = \left(n+\frac{1}{2}\right)\delta\omega_r^{(i)} + \sum_{j\neq i}\frac{g_{i,j}^2}{2}\left(\frac{1}{\omega_{ij}-\omega_r} - \frac{1}{\omega_{ij}+\omega_r}\right), \tag{5}$$

where the shift $\delta\omega_r^{(i)}$ of the resonator frequency reads

$$\delta\omega_r^{(i)} = \lambda^2\omega''_i + \sum_{j\neq i} g_{i,j}^2\left(\frac{2}{\omega_{ij}} - \frac{1}{\omega_{ij}-\omega_r} - \frac{1}{\omega_{ij}+\omega_r}\right), \tag{6}$$

with $\hbar g_{i,j} = \lambda|\langle\Phi_i|\hat{H}'_{\rm qc}|\Phi_j\rangle|$ the coupling strength between states i and j, $\omega_i = E_i/\hbar$ and $\omega_{ij} = \omega_j - \omega_i$. Equations (5) and (6) are the main results of this work, in particular Eq. (6) contains both the adiabatic and the dispersive contributions to the resonator shift, as explained below. In the classical limit, it can be related to the real part of the ac current susceptibility as calculated in Ref. [20] for a fermionic system in thermal equilibrium.

The ω_r-independent terms on the right-hand side of Eq. (6) are the contributions involving $\hat{H}''_{\rm qc}$ that arise from Eq. (4), while the ω_r-dependent terms correspond to those obtained from a multilevel Jaynes-Cummings Hamiltonian. It can be seen from Eq. (6) that all transitions which couple a given state i with other states j via $\hat{H}'_{\rm qc}$ are relevant to calculate the shift $\delta\omega_r^{(i)}$ of the resonance frequency. The equation includes the contribution both from virtual transitions that do not depend on the resonator and from transitions mediated by the absorption and emission of photons. Equation (6) only holds far from resonances, i.e., when all transitions between states of the circuit have energies that differ from ω_r by much more than the coupling energy.

In the limit where $\omega_r \ll \omega_{ij}$ for all transitions, Eq. (6) simplifies to $\delta\omega_r^{(i)} \approx \delta\omega_r^{\rm curv} = \lambda^2\omega''_i$, corresponding to a frequency shift proportional to the curvature of the energy level with x. Noting that, for a charge-parameter q, $(\partial^2 E_i/\partial q^2)^{-1}$ is the effective capacitance [21] of the circuit in state i, and for a phase-parameter φ, $(\Phi_0/2\pi)^2(\partial^2 E_i/\partial\varphi^2)^{-1}$ its effective inductance (here Φ_0 is the flux quantum), this limit finds a simple interpretation: the resonator capacitance or inductance is merely renormalized by that of the quantum circuit.

It is only in the case where terms from $H''_{\rm qc}$ are negligible that one recovers the result that can be derived from the generalized Jaynes-Cummings Hamiltonian [22], in which the frequency shift is dominated by the contributions involving the exchange of excitations

$$\delta\omega_r^{(i)} \approx \delta\omega_r^{\rm JC} = -\sum_{j\neq i} g_{i,j}^2\left(\frac{1}{\omega_{ij}-\omega_r} + \frac{1}{\omega_{ij}+\omega_r}\right). \tag{7}$$

In the following, we will use the shortcut "JC" for this contribution. For a quantum circuit described by a two-level system $\{|0\rangle, |1\rangle\}$, this result was derived from the Jaynes-Cummings Hamiltonian in the dispersive limit beyond the rotating-wave approximation (RWA) in Refs. [3,6]. Assuming $g_{01} \ll |\omega_{01}-\omega_r| \ll \omega_{01}+\omega_r$, it simplifies to $\delta\omega_r^{(0/1)} \sim \mp g_{01}^2/(\omega_{01}-\omega_r)$, which is the cavity-pull χ_{01} in the RWA [4]. When restricting to the three lowest energy levels of a multilevel circuit, Eq. (6) also allows us to recover the shifts derived for the transmon in the RWA in Ref. [22]: $\delta\omega_r^{(0)} \approx -\chi_{01}$, $\delta\omega_r^{(1)} \approx \chi_{01} - \chi_{12}$, and $\chi_{ij} = g_{ij}^2/(\omega_{ij}-\omega_r)$.

Altogether, Eq. (6) shows that the curvature of the energy levels, i.e., the effective admittance of the circuit, is actually a distinct contribution to the shift and can be described on the same footing as the cavity pull given by the Jaynes-Cummings Hamiltonian. This result clarifies a link between both that had been suggested in early works [3,4].

Short weak link.—As a first example we address the case of a resonator inductively coupled to a small loop closed through a short, single-channel superconducting weak link. In a simplified low-energy description and neglecting the presence of excess quasiparticles, this circuit is characterized by two levels, at energies $\omega_0 = -E_A/\hbar$ and $\omega_1 = E_A/\hbar$, with $E_A = \Delta\sqrt{1-\tau\sin^2(\delta/2)}$, the Andreev energy, Δ the superconducting gap, τ the channel transmission, and δ the phase across the weak link [23–25]. The sole matrix element required to calculate the frequency shifts adopts the following analytical form [26,27]

$$\langle 0|H'|1\rangle = \frac{\Delta\sqrt{1-\tau}}{2}\left(\frac{\Delta}{E_A} - \frac{E_A}{\Delta}\right). \tag{8}$$

We show in Fig. 1, for $\tau = 0.8$, and three values of the resonator frequency ω_r, the phase dependence of the resonator frequency shift $\delta\omega_r^{(0)}$ when the Andreev system is in its ground state. In Fig. 1(d), $\omega_r = 0.1\Delta/\hbar$ is much smaller than ω_{01} at all phases, and $\delta\omega_r^{(0)}$ is precisely given by the term associated to the curvature $\lambda^2\omega_0''$. In Fig. 1(f), $\omega_r = 0.7\Delta/\hbar$ approaches ω_{01} at $\delta \approx \pi$, so that the shift is in this region very close to the JC contribution, whereas further from π it is given by the curvature. In Fig. 1(e), $\omega_r = 1.2\Delta/\hbar$ crosses ω_{01}, and the characteristic anticrossing behavior in $\delta\omega_r^{(0)}$ can be observed, well described by JC. Away from $\delta \approx \pi$, the curvature once again takes over. While the short junction limit provides a simple analytical example to illustrate the crossover from the adiabatic to the dispersive regimes, a richer behavior, including finite length, parity, and spin-orbit effects [17,28,29], will be analyzed elsewhere [30].

rf-SQUID.—To illustrate our result from Eq. (6) in a multilevel situation, we now address the rf-SQUID, used in particular as a simple flux qubit [31,32]. Its Hamiltonian reads

$$H = 4E_C\hat{N}^2 + \frac{E_L}{2}\hat{\varphi}^2 - E_J\cos\left(\hat{\varphi} + 2\pi\frac{\Phi_e}{\Phi_0}\right), \tag{9}$$

where $\hat{N}$ is the number of Cooper pairs having crossed the Josephson junction, $\hat{\varphi}$ the phase across the loop inductance, $E_C = e^2/2C$ the charging energy, E_J the Josephson energy and $E_L = \Phi_0^2/4\pi^2 L$ the magnetic energy associated with the loop geometric inductance L. The external flux Φ_e threading the loop is the control parameter. By numerical diagonalization of the Hamiltonian, we obtain the spectrum, shown in Fig. 2(b) for $E_L = E_C = E_J/5$, and the

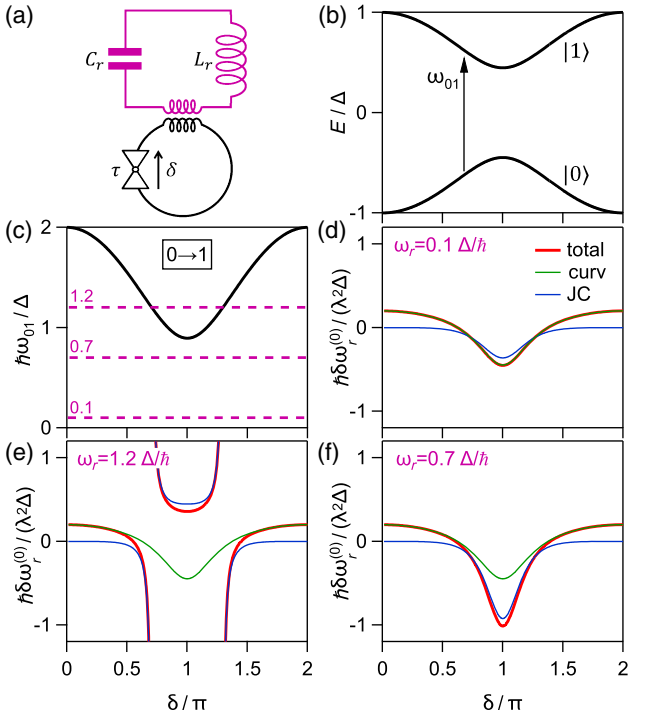

FIG. 1. Short single-channel weak link. (a) Circuit layout: the loop containing the phase-biased weak link of transmission τ is coupled to a microwave resonator (top). (b) Phase-dependence of the energy levels for $\tau = 0.8$. (c) Transition energy $\hbar\omega_{01} = 2E_A$; (d),(e),(f) resonator frequency shift in ground state $\delta\omega_r^{(0)}$ as a function of phase δ across weak link, for three values of the resonator frequency indicated with magenta dashed lines in (c). Red line: total shift; green line: curvature contribution; blue line: JC contribution [Eq. (7)].

transition energies ω_{0j} from state $|0\rangle$ [Fig. 2(c)] and ω_{1j} from state $|1\rangle$ [Fig. 2(d)]. The resonator frequency shifts $\delta\omega_r^{(0,1)}$ when the circuit is in $|0\rangle$ or $|1\rangle$ are shown in Figs. 2(e) and 2(f), for a resonator at $\omega_r = 0.3E_J/\hbar$. The curvature and JC contributions are shown as green and blue lines, respectively. It is only close to the crossings $\omega_{01} \approx \omega_r$ ($\omega_{12} \approx \omega_r$) that $\delta\omega_r^{(0,1)}$ coincide with the JC contribution. When $\omega_r \ll \omega_{01}$ ($\omega_r \ll \omega_{12}, \omega_{01}$), the contribution from the curvature almost coincides with the total shift. When none of these conditions is met, the complete formula is necessary to describe the frequency shift, as clearly seen in Figs. 2(e) and 2(f). However, if $8\lambda^2 E_C \ll \hbar\omega_{01}$, then the JC expression is almost correct if one uses an effective resonator frequency $\hbar\omega_r^{\text{eff}} = \hbar\omega_r + 8\lambda^2 E_C$.

Cooper pair box.—We now consider the Cooper pair box, a circuit that has both been discussed from the adiabatic [11,12,14] and from the dispersive [4,22] point of view. Its Hamiltonian reads

$$H_{\text{cpb}} = 4E_C(\hat{N} - N_g)^2 - E_J\cos\hat{\varphi}, \tag{10}$$

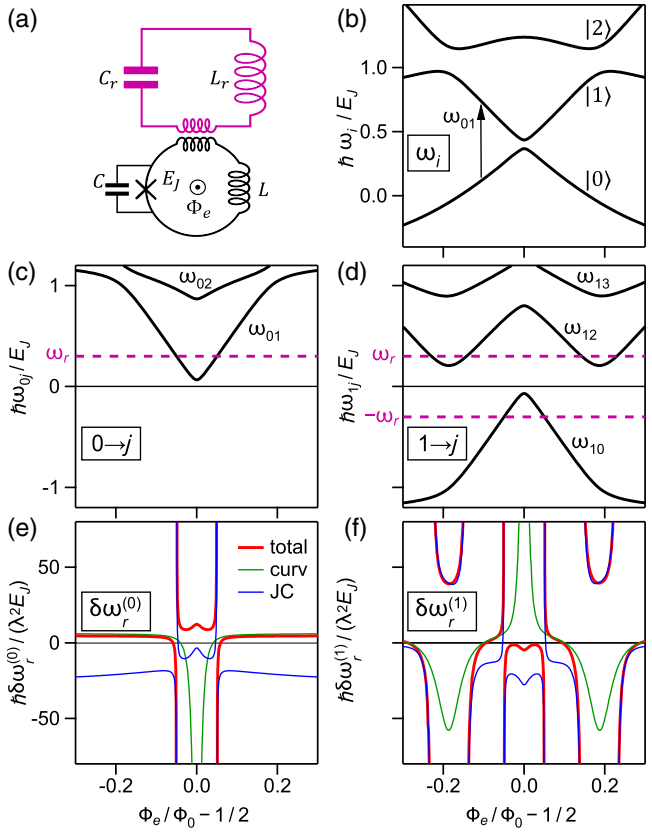

FIG. 2. rf-SQUID. (a) Schematics of the circuit, consisting of a Josephson junction with Josephson energy E_J and capacitance C, inserted in a loop with inductance L threaded by a magnetic flux Φ_e, and coupled to a microwave resonator (top). (b) Spectrum calculated using $E_C = E_L = E_J/5$. (c),(d) Transition energy ω_{0i} (ω_{1i}) from $|0\rangle$ ($|1\rangle$). (e),(f) Resonator frequency shift $\delta\omega_r^{(0)}$ ($\delta\omega_r^{(1)}$) as a function of $\Phi_e/\Phi_0 - 1/2$, for resonator placed at $\omega_r = 0.3E_J/\hbar$ [magenta dashed lines in (c),(d)]. Red line: total shift; blue line: JC contribution; green line: curvature contribution.

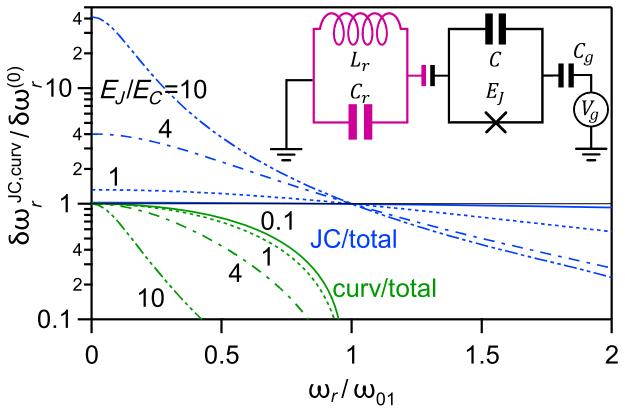

FIG. 3. Cooper pair box. Ratio of JC ($\delta\omega_r^{\rm JC}$, blue) and curvature ($\delta\omega_r^{\rm curv} = \lambda^2\omega_0''$, green) contributions to total resonator frequency shift $\delta\omega_r^{(0)}$, at $N_g = C_gV_g/2e = 1/2$, for $E_J/E_C = 0.1$, 1, 4, and 10, as a function of resonator frequency ω_r normalized to transition frequency ω_{01}. Inset: schematics of the Cooper pair box (black) coupled to microwave resonator (magenta).

with now $\hat{\varphi}$ being the phase across the Josephson junction, conjugated to $\hat{N}$, and N_g being the reduced gate voltage (see inset in Fig. 3).

In this case, $\lambda^2 H''_{\rm cpb} = 8\lambda^2 E_C$ is a constant which, when added to the JC contribution, leads to the N_g-dependent shift $\lambda^2\omega_i''$ in the limit $\omega_r \to 0$. This is illustrated in Fig. 3, showing the ratio of the JC and curvature contribution to the total frequency shift as a function of ω_r, when the circuit is in state $|0\rangle$, at $N_g = 1/2$ and for various values of E_J/E_C. At $\omega_r \ll \omega_{01}$, the JC result overestimates by far the shift, and $\delta\omega_r^{(0)}$ is given by the curvature (adiabatic regime): $\delta\omega_r^{\rm curv}/\delta\omega_r^{(0)} \approx 1$. Around the anticrossing at $\omega_r = \omega_{01}$, the JC contribution becomes very large, so that the constant contribution $8\lambda^2 E_C$ is relatively negligible (dispersive regime): $\delta\omega_r^{\rm JC}/\delta\omega_r^{(0)} \approx 1$. When $E_J/E_C \lesssim 1$, the JC result is very close to the exact result for all resonator frequencies. In contrast, for $E_J/E_C \gg 1$, the limiting expressions $\delta\omega_r^{\rm curv}$ and $\delta\omega_r^{\rm JC}$ are only valid at $\omega_r \approx 0$ and $\omega_r \approx \omega_{01}$, respectively. Between these two limits the complete expression of Eq. (6) is needed to account for the frequency shift.

Conclusion and outlook.—We have introduced a formulation of circuit QED readout bridging between the adiabatic and the dispersive limits that have been used to describe the coupling of a quantum circuit to a resonator in different regimes. While we have illustrated our work by considering simple models, it provides a means to describe quantitatively circuit QED experiments which explore large ranges of transition frequencies [10,17]. In particular, this is of importance for the spectroscopy of mesoscopic systems, like quantum hybrid devices combining spin-active materials (strong spin-orbit semiconducting nanowires or two-dimensional electron gases, topological insulators, etc.) and superconductors, currently explored in quest of topological superconductivity.

We thank our colleagues from the Quantronics group for useful discussions. This work has been supported by ANR contract JETS, by FET-Open contract AndQC, by the Spanish MINECO through Grants No. FIS2014-55486-P and No. FIS2017-84860-R and through the "María de Maeztu" Programme for Units of Excellence in R&D (Grant No. MDM-2014-0377). S. P. acknowledges support by "Doctor Banco Santander-María de Maeztu" program. L. T. was supported by the Marie Skłodowska-Curie individual fellowship Grant No. 705467, and C. M. by Region Ile-de-France in the framework of DIM SIRTEQ.

S. P., C. M., and L. T. contributed equally to this work.

*Corresponding author.
a.l.yeyati@uam.es

[1] A. Blais, S. M. Girvin, and W. D. Oliver, Quantum information processing and quantum optics with circuit quantum electrodynamics, Nat. Phys. **16**, 247 (2020).

[2] A. A. Clerk, K. W. Lehnert, P. Bertet, J. R. Petta, and Y. Nakamura, Hybrid quantum systems with circuit quantum electrodynamics, Nat. Phys. **16**, 257 (2020).
[3] G. Johansson, L. Tornberg, V. S. Shumeiko, and G. Wendin, Readout methods and devices for Josephson-junction-based solid-state qubits, J. Phys. Condens. Matter **18**, S901 (2006).
[4] A. Blais, R-S. Huang, A. Wallraff, S. M. Girvin, and R. J. Schoelkopf, Cavity quantum electrodynamics for superconducting electrical circuits: An architecture for quantum computation, Phys. Rev. A **69**, 062320 (2004).
[5] A. Wallraff, D. I. Schuster, A. Blais, L. Frunzio, R.- S. Huang, J. Majer, S. Kumar, S. M. Girvin, and R. J. Schoelkopf, Strong coupling of a single photon to a superconducting qubit using circuit quantum electrodynamics, Nature (London) **431**, 162 (2004).
[6] D. Zueco, G. M. Reuther, S. Kohler, and P. Hänggi, Qubit-oscillator dynamics in the dispersive regime: Analytical theory beyond the rotating-wave approximation, Phys. Rev. A **80**, 033846 (2009).
[7] W. C. Smith, A. Kou, U. Vool, I. M. Pop, L. Frunzio, R. J. Schoelkopf, and M. H. Devoret, Quantization of inductively shunted superconducting circuits, Phys. Rev. B **94**, 144507 (2016).
[8] S. Kohler, Dispersive readout: Universal theory beyond the rotating-wave approximation, Phys. Rev. A **98**, 023849 (2018).
[9] M. H. Ansari, Superconducting qubits beyond the dispersive regime, Phys. Rev. B **100**, 024509 (2019).
[10] G. Zhu, D. G. Ferguson, V. E. Manucharyan, and J. Koch, Circuit QED with fluxonium qubits: Theory of the dispersive regime, Phys. Rev. B **87**, 024510 (2013).
[11] M. A. Sillanpää, T. Lehtinen, A. Paila, Yu. Makhlin, L. Roschier, and P. J. Hakonen, Direct Observation of Josephson Capacitance, Phys. Rev. Lett. **95**, 206806 (2005).
[12] T. Duty, G. Johansson, K. Bladh, D. Gunnarsson, C. Wilson, and P. Delsing, Observation of Quantum Capacitance in the Cooper-Pair Transistor, Phys. Rev. Lett. **95**, 206807 (2005).
[13] M. A. Sillanpää, L. Roschier, and P. J. Hakonen, Inductive Single-Electron Transistor, Phys. Rev. Lett. **93**, 066805 (2004).
[14] A. Paila, D. Gunnarsson, J. Sarkar, M. A. Sillanpää, and P. J. Hakonen, Current-phase relation and Josephson inductance in a superconducting Cooper-pair transistor, Phys. Rev. B **80**, 144520 (2009).
[15] F. Persson, C. M. Wilson, M. Sandberg, and P. Delsing, Fast readout of a single Cooper-pair box using its quantum capacitance, Phys. Rev. B **82**, 134533 (2010).
[16] M. T. Bell, L. B. Ioffe, and M. E. Gershenson, Microwave spectroscopy of a Cooper-pair transistor coupled to a lumped-element resonator, Phys. Rev. B **86**, 144512 (2012).
[17] L. Tosi, C. Metzger, M. F. Goffman, C. Urbina, H. Pothier, Sunghun Park, A. Levy Yeyati, J. Nygárd, and P. Krogstrup, Spin-Orbit Splitting of Andreev States Revealed by Microwave Spectroscopy, Phys. Rev. X **9**, 011010 (2019).
[18] See the Supplemental Material http://link.aps.org/supplemental/10.1103/PhysRevLett.125.077701 for the derivation of Eqs. (5) and (6) and for the coupling scheme between a resonator and a quantum circuit, which includes Ref. [19].
[19] L. Bretheau, Localized excitations in superconducting atomic contacts; probing the Andreev doublet, Ph. D. thesis, Ecole Polytechnique, 2013, https://tel.archives-ouvertes.fr/pastel-00862029#.
[20] M. Trif, O. Dmytruk, H. Bouchiat, R. Aguado, and P. Simon, Dynamic current susceptibility as a probe of Majorana bound states in nanowire-based Josephson junctions, Phys. Rev. B **97**, 041415(R) (2018).
[21] D. V. Averin and C. Bruder, Variable Electrostatic Transformer: Controllable Coupling of Two Charge Qubits, Phys. Rev. Lett. **91**, 057003 (2003).
[22] J. Koch, T. M. Yu, J. Gambetta, A. A. Houck, D. I. Schuster, J. Majer, A. Blais, M. H. Devoret, S. M. Girvin, and R. J. Schoelkopf, Charge-insensitive qubit design derived from the Cooper pair box, Phys. Rev. A **76**, 042319 (2007).
[23] C. W. J. Beenakker and H. van Houten, Josephson Supercurrent through a Superconducting Quantum Point Contact Shorter than the Coherence Length, Phys. Rev. Lett. **66**, 3056 (1991).
[24] A. Furusaki and M. Tsukada, Dc Josephson effect and Andreev reflection, Solid State Commun. **78**, 299 (1991).
[25] P. F. Bagwell, Suppression of the Josephson current through a narrow, mesoscopic, semiconductor channel by a single impurity, Phys. Rev. B **46**, 12573 (1992).
[26] A. Zazunov, A. Brunetti, A. Levy Yeyati, and R. Egger, Quasiparticle trapping, Andreev level population dynamics, and charge imbalance in superconducting weak links, Phys. Rev. B **90**, 104508 (2014).
[27] C. Janvier, L. Tosi, L. Bretheau, Ç. Ö. Girit, M. Stern, P. Bertet, P. Joyez, D. Vion, D. Esteve, M. F. Goffman, H. Pothier, and C. Urbina, Coherent manipulation of Andreev states in superconducting atomic contacts, Science **349**, 1199 (2015).
[28] S. Park and A. Levy Yeyati, Andreev spin qubits in multichannel Rashba nanowires, Phys. Rev. B **96**, 125416 (2017).
[29] M. Hays, V. Fatemi, K. Serniak, D. Bouman, S. Diamond, G. de Lange, P. Krogstrup, J. Nygrd, A. Geresdi, and M. H. Devoret, Continuous monitoring of a trapped superconducting spin, Nat. Phys., https://doi.org/10.1038/s41567-020-0952-3 (2020).
[30] C. Metzger, S. Park, L. Tosi, A. A. Reynoso, M. F. Goffman, C. Urbina, A. Levy Yeyati, and H. Pothier, Circuit-QED with phase-biased Josephson weak links (to be published).
[31] J. R. Friedman, V. Patel, W. Chen, S. K. Tolpygo, and J. E. Lukens, Quantum superposition of distinct macroscopic states, Nature (London) **406**, 43 (2000).
[32] M. H. Devoret, A. Wallraff, and J. M. Martinis, Superconducting qubits: A short review, arXiv:cond-mat/0411174.